ARMY RESEARCH LABORATORY

INFRARED TRANSMISSION AND PATH RADIANCE THROUGH DUST AND FOG

James Williams

ARL-MR-35

April 1993

NOTICES

Disclaimers

The findings in this report are not to be construed as an official Department of the Army position, unless so designated by other authorized documents.

The citation of trade names and names of manufacturers in this report is not to be construed as official Government indorsement or approval of commercial products or services referenced herein.

Destruction Notice

When this document is no longer needed, destroy it by any method that will prevent disclosure of its contents or reconstruction of the document.

REPORT DOCUMENTATION PAGE

Form Approved
OMB No 0704-0188

1. AGENCY USE ONLY *(Leave blank)*	2. REPORT DATE	3. REPORT TYPE AND DATES COVERED
	April 1993	Final

4. TITLE AND SUBTITLE
INFRARED TRANSMISSION AND PATH RADIANCE THROUGH DUST AND FOG

5. FUNDING NUMBERS
62784/AH71

6. AUTHOR(S)
James Williams

7. PERFORMING ORGANIZATION NAME(S) AND ADDRESS(ES)
U.S. Army Research Laboratory
Battlefield Environment Directorate
ATTN: AMSRL-BE-M
White Sands Missile Range, NM 88002-5501

8. PERFORMING ORGANIZATION REPORT NUMBER
ARL-MR-35

9. SPONSORING/MONITORING AGENCY NAME(S) AND ADDRESS(ES)
U.S. Army Research Laboratory
2800 Powder Mill Road
Adelphi, MD 20783-1145

10. SPONSORING/MONITORING AGENCY REPORT NUMBER

11. SUPPLEMENTARY NOTES

12a. DISTRIBUTION/AVAILABILITY STATEMENT
Approved for public release; distribution unlimited.

12b. DISTRIBUTION CODE

13. ABSTRACT *(Maximum 200 words)*

The obscurant effects of dust and fog can significantly degrade the performance of infrared (IR) sensors engaged in target acquisition. To quantify these effects, computer runs were conducted using the EOSAEL model FCLOUD for the 3- to 5-μm and 8- to 12-μm wavebands. FCLOUD was used to calculate beam transmission and path radiance through homogeneous ellipsoidal dust and fog clouds. Both advective and radiation fogs were considered. The EOSAEL models XSCALE and LOWTRAN 7 were also run to calculate transmission over the same wavebands for fog. These results compare favorably with FCLOUD.

This study suggests that the performance of IR sensors in the wavebands investigated will be severely degraded in the presence of heavy or moderate fog. Under the dust conditions studied, IR transmission is considerably better than for fog. There is an expected transmission loss, however, with the inclusion of multiple scattering effects and a progressively greater loss as the cloud path length increases.

14. SUBJECT TERMS
infrared, transmission, path radiance, dust, fog

15. NUMBER OF PAGES
29

16. PRICE CODE

17. SECURITY CLASSIFICATION OF REPORT	18. SECURITY CLASSIFICATION OF THIS PAGE	19. SECURITY CLASSIFICATION OF ABSTRACT	20. LIMITATION OF ABSTRACT
Unclassified	Unclassified	Unclassified	SAR

NSN 7540-01-280-5500

Standard Form 298 (Rev. 2-89)

Contents

Figures

1. Introduction

This work was undertaken to assess the effects of dust and fog on generic terminal-homing infrared (IR) sensors. Transmission and path radiance effects for the mid- and far-IR wavebands were evaluated by using the EOSAEL computer models FCLOUD [Turner 1987], XSCALE [Fiegel 1992], and LOWTRAN 7 [Kneizys et al. 1989]. Note that the figures in this document refer to σ, which is the Beer's law extinction coefficient. All extinctions should be interpreted as IR extinctions.

2. Computer Models and Scenarios

The primary model used for this study was FCLOUD because of its ability to calculate path radiance and transmittance through dust and fog clouds. The IR wavebands of interest were 3 to 5 μm and 8 to 12 μm. Path radiance calculations (in watts per meter^2-steradian-micrometer) were in terms of thermal emission, scattering, and total path radiance. For nearly all runs, the thermal path radiance comprised well over 90 percent of the total path radiance. This report presents only the total path radiance results.

FCLOUD computer runs were initially performed to generate transmission and path radiance data for 200-m path lengths through moderate fog, heavy fog, and heavy dust. These runs used extinction coefficients retrieved from the Phase Function Data Base model PFNDAT [Shirkey et al. 1987]. The phase function identifiers used were 25 for heavy fog, 26 for moderate fog, and 51 for heavy loading dust. The heavy and moderate fog models used by PFNDAT were taken from the work of Shettle and Fenn [1979]. The visibilities associated with these models are 130 m for heavy fog and 450 m for moderate fog. For heavy fog, the particle mode radius is 10.0 μm with a number density of 20 particles/cm^3; for moderate fog, the mode radius is 2.0 μm with a number density of 200 particles/cm^3. As a means of comparison with FCLOUD, the models XSCALE and LOWTRAN 7 were then run to calculate transmission for moderate and heavy fog. LOWTRAN 7 was set up to use the default model visibiliti[illegible]00 m for moderate fog and 200 m for heavy fog. The XSCALE transmission runs used visibilities identical to those of FCLOUD in an attempt to provide a better comparison with the FCLOUD results. All of the first set of runs assumed a 200-m path length, single scattering, and a solar zenith angle of 45 degrees. Additional FCLOUD multiple scattering calculations were made over an 800-m path and solar angle of 15 degrees.

In addition to moderate and heavy fog clouds, heavy loading dust clouds were considered for this study. Such a dust consists of particles with a bimodal size distribution that ranges from a fraction of a micron for the small mode to well over 10 μm for the large mode [Shirkey et al. 1987]. The number density was taken to be approximately 189 particles/cm^3 (comprised overwhelmingly of small-mode particles).

Note that the visibilities given for dust in figures 1–4 and figures 25–34 were derived from the Koschmieder equation

$$V = \frac{3.912}{\beta} \quad (1)$$

where V is the visibility (meteorological range) in kms and β is the visible extinction coefficient. The visibility of 2.5 km for the dust runs that used PFNDAT (shown in figures 1–4 and figures 29–30) was derived by using the visible extinction for heavy dust given in table 1 of Shirkey et al. [1987]. The visibilities for the remaining dust figures were estimated by assuming the visible extinctions were a close approximation to the given IR extinctions. These values were then used directly in the Koschmieder equation. This assumption is valid and is justified by noting that the extinctions for heavy dust show little variability from the visible to the far-IR (table 1 of Shirkey et al. 1987). This characteristic of neutral extinction for heavy dust has also been observed by Jennings, Pinnick, and Auvermann [1978] and by Pinnick, Fernandez, and Hinds [1983].

For *all* computer runs, unless otherwise noted, the following input parameters were used.

- Clouds were assumed to be at ground level with source and receiver positions at opposite ends of the cloud.
- cloud temperature 15° C.
- atmospheric temperature 20° C.
- atmospheric IR optical thickness 0.38 (FCLOUD model).
- background surface albedo 0.5.
- background radiance (watts per meter^2-steradian-micrometer) calculated by FCLOUD.

- solar zenith angle 45 degrees (15 degrees for all multiple scattering runs).

- solar azimuth angle of 270 degrees.

- lunar day set to zero, thus only solar irradiance was calculated.

FCLOUD by default uses a relatively low IR extinction for heavy dust (approximately 1.5 km^{-1}). Therefore, the following additional FCLOUD dust runs were made using extinctions of 3.0 and 4.0 km^{-1}.

- Path radiance. Single scattering. Solar zenith angle of 45 degrees. 200-m path length.

- Path radiance. Multiple scattering. Solar zenith angle of 15 degrees. 800-m path length.

- Transmittance. Multiple scattering. Solar zenith angle of 15 degrees. 800-m path length.

3. Results

3.1 FCLOUD Calculations for Dust and Fog

Figures 1 through 12 show FCLOUD path radiance and transmission results using extinction coefficients stored in PFNDAT. The FCLOUD computer runs assumed single scattering, a solar zenith angle of 45 degrees, and a 200-m path length. Note that the extinction coefficient given for each figure is the average for that waveband; the actual extinctions vary according to the calculations performed in PFNDAT based on the sensor's wavelength response. The figures clearly indicate that IR transmission through fog is greatly attenuated. The attenuation due to dust would be considered moderate.

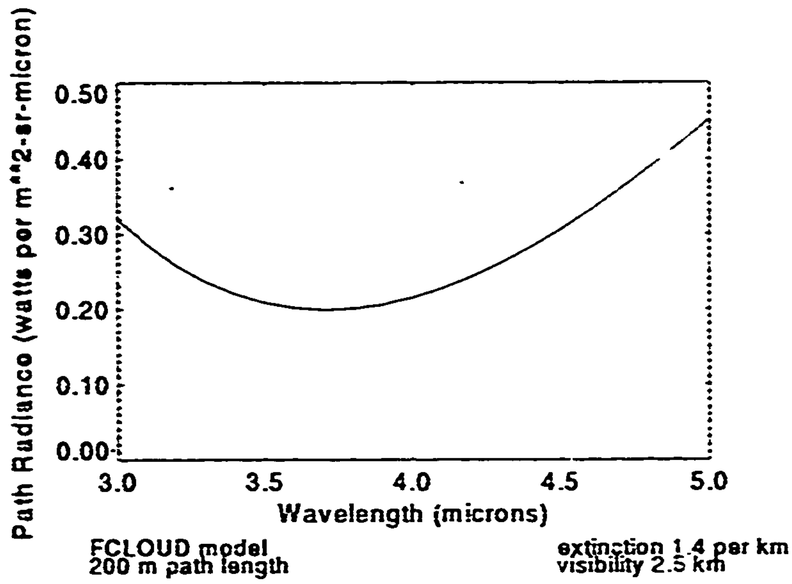

Figure 1: Dust path radiance (mid IR, $\sigma = 1.4$ km^{-1})

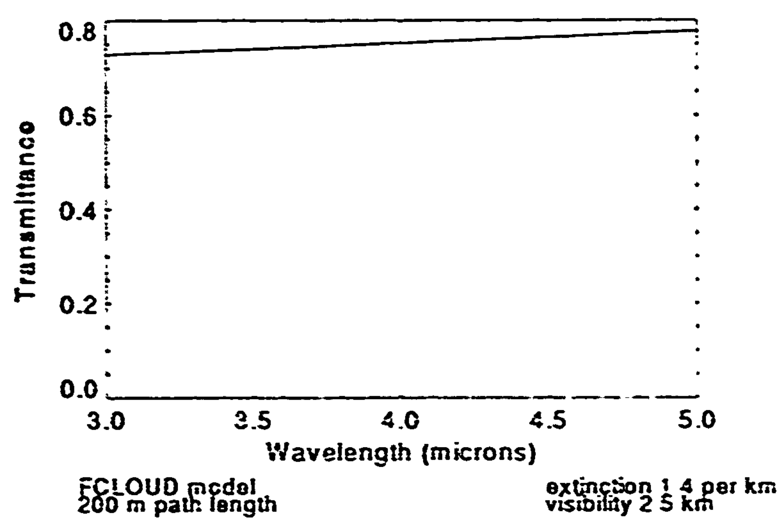

Figure 2: Dust transmittance (mid IR, $\sigma = 1.4$ km^{-1})

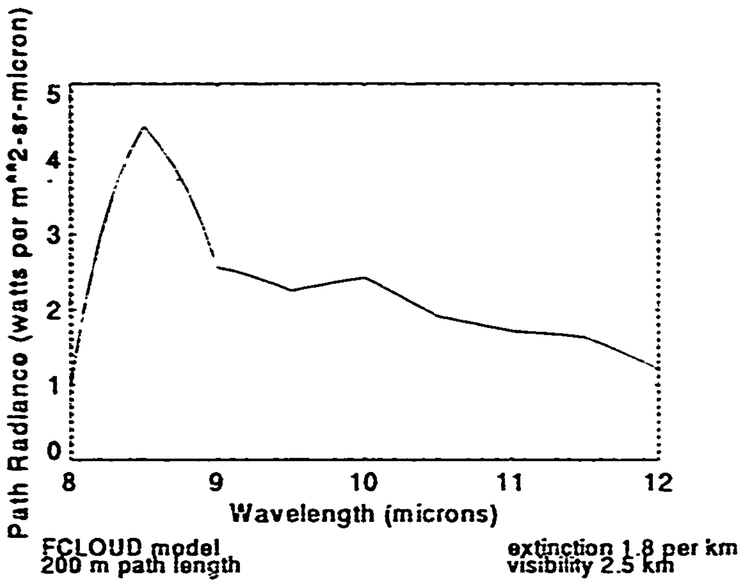

Figure 3: Dust path radiance (far IR, $\sigma = 1.8\ km^{-1}$)

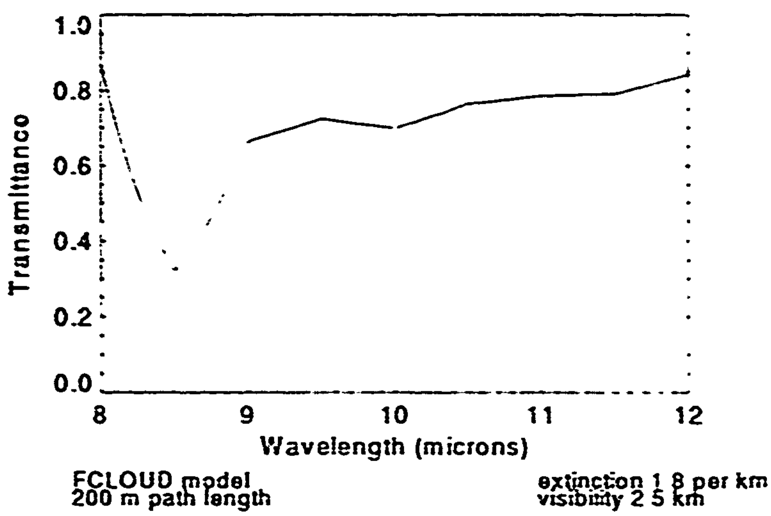

Figure 4: Dust transmittance (far IR, $\sigma = 1.8\ km^{-1}$)

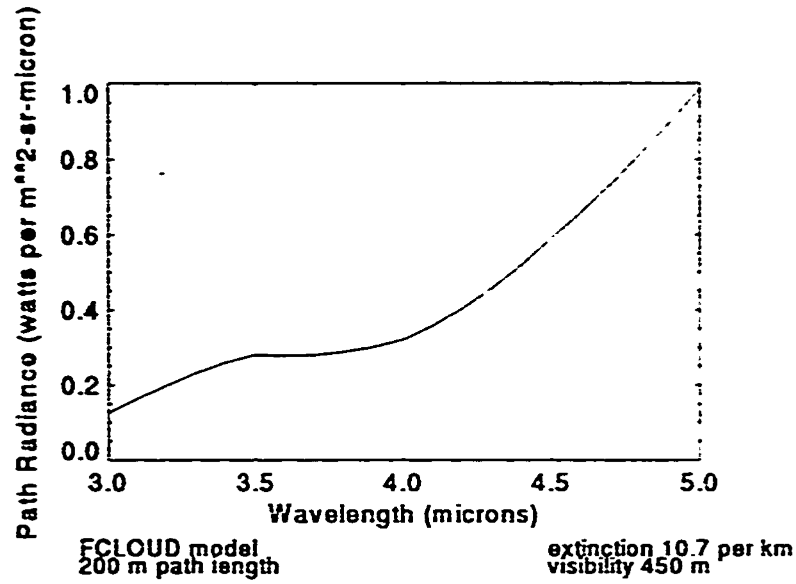

Figure 5: Moderate fog path radiance (mid IR. σ = 10.7 km^{-1})

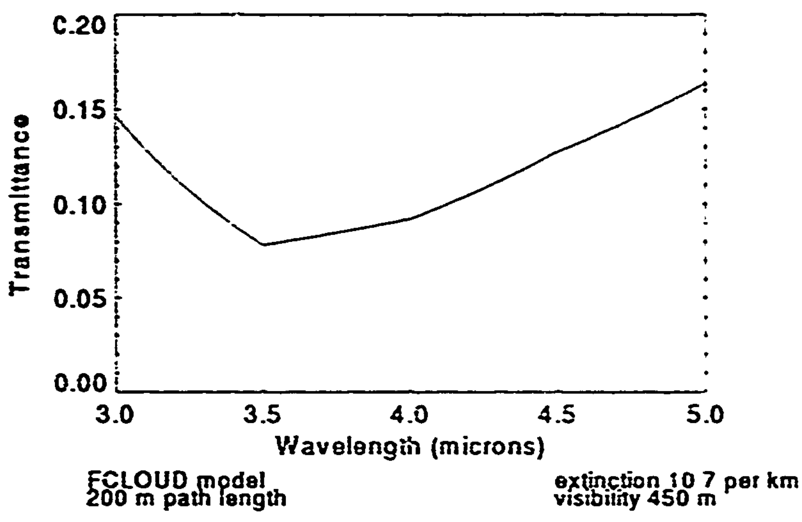

Figure 6: Moderate fog transmittance (mid IR. σ = 10.7 km^{-1})

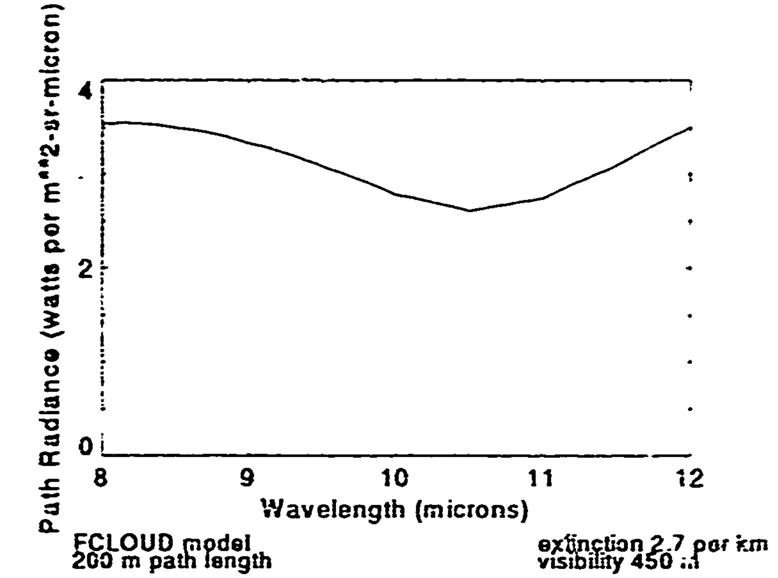

Figure 7: Moderate fog path radiance (far IR, $\sigma = 2.7\ km^{-1}$)

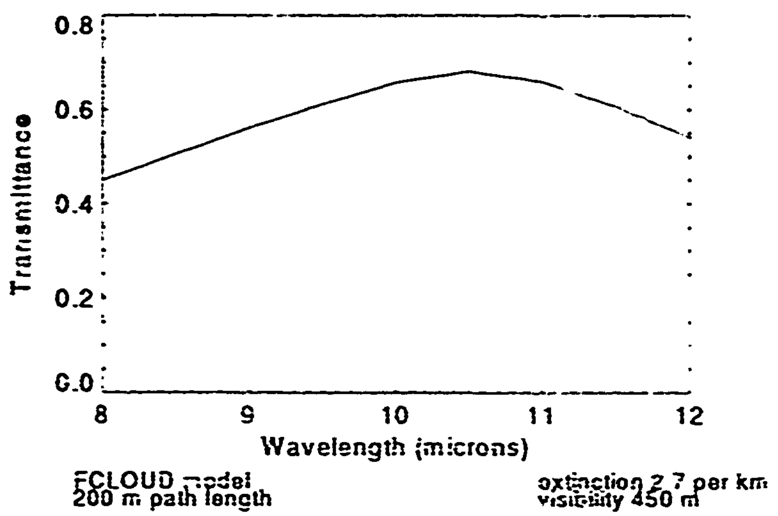

Figure 8: Moderate fog transmittance (far IR, $\sigma = 2.7\ km^{-1}$)

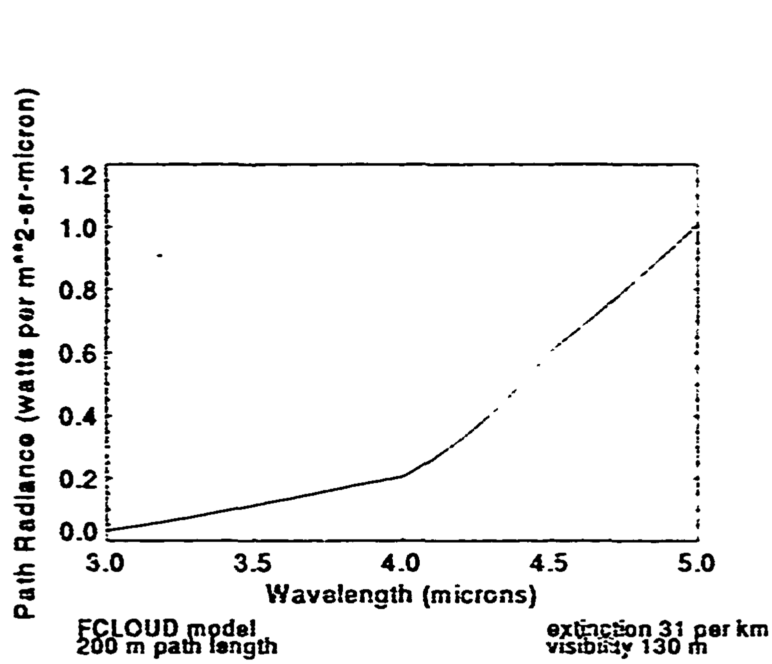

Figure 9: Heavy fog path radiance (mid IR, $\sigma = 31\ \text{km}^{-1}$)

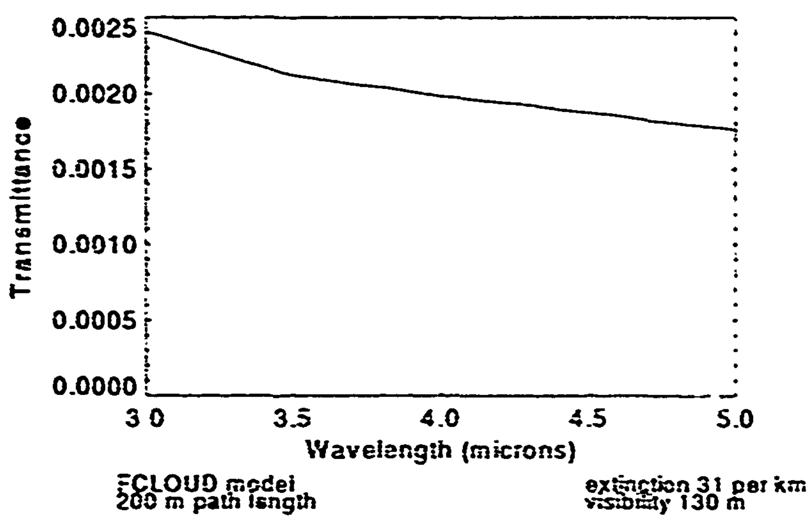

Figure 10: Heavy fog transmittance (mid IR, $\sigma = 31\ \text{km}^{-1}$)

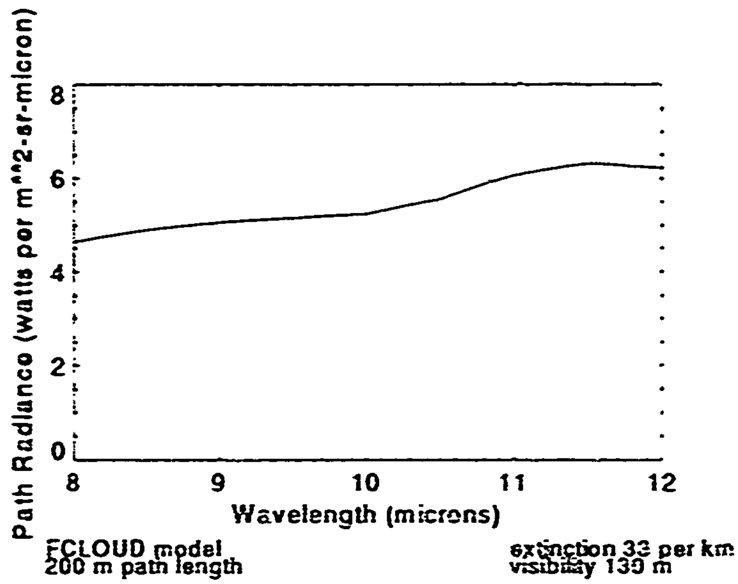

Figure 11: Heavy fog path radiance (far IR. $\sigma = 33\ km^{-1}$)

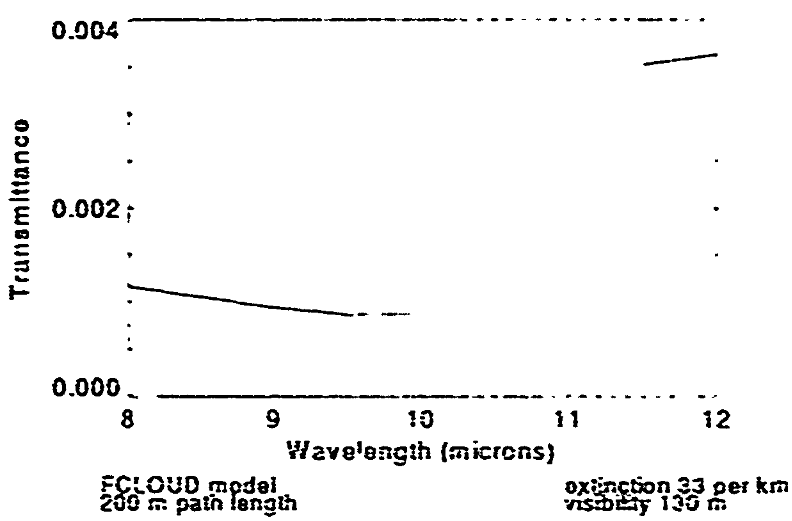

Figure 12: Heavy fog transmittance (far IR. $\sigma = 33\ km^{-1}$)

3.2 LOWTRAN 7 and XSCALE Transmission Results for Fog

Figures 13 through 20 show LOWTRAN 7 and XSCALE transmission results for moderate and heavy fog. Note that LOWTRAN 7 superimposes the aerosol effects on the attentuation caused by atmospheric gases. LOWTRAN 7 was run using the default visibilities (500 m for moderate fog and 200 m for heavy fog). The XSCALE runs used visibilities identical to those of FCLOUD to provide a better means of comparison.

Figures 21 through 24 directly compare the FCLOUD results with those of LOWTRAN 7 and XSCALE. The models show the same general level of transmittance across each waveband. Both FCLOUD and XSCALE use the fog models of Shettle and Fenn, thus the results produced by each are nearly identical. The falloff at 4.3 μm for LOWTRAN 7 is due to absorption by molecular CO_2. The higher transmittance shown in figures 23 and 24 for LOWTRAN 7 as compared to FCLOUD and XSCALE is a function of the significantly higher visibility of 200 m used by the LOWTRAN 7 model for heavy fog conditions.

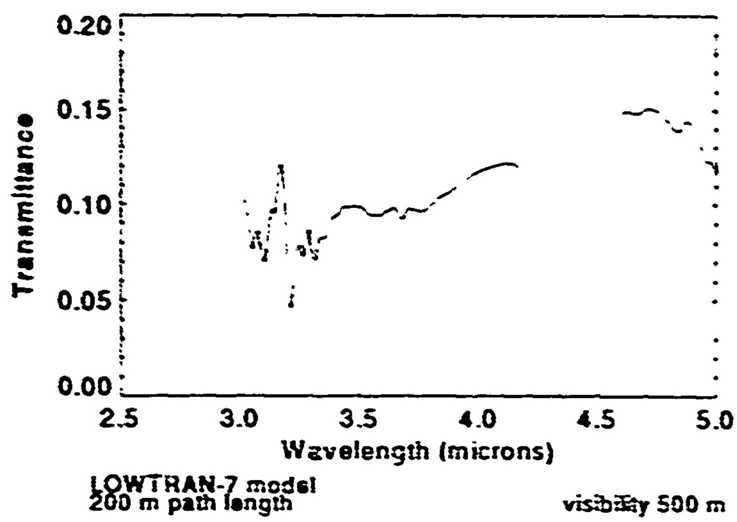

Figure 13: Moderate fog transmittance (LOWTRAN 7, mid IR)

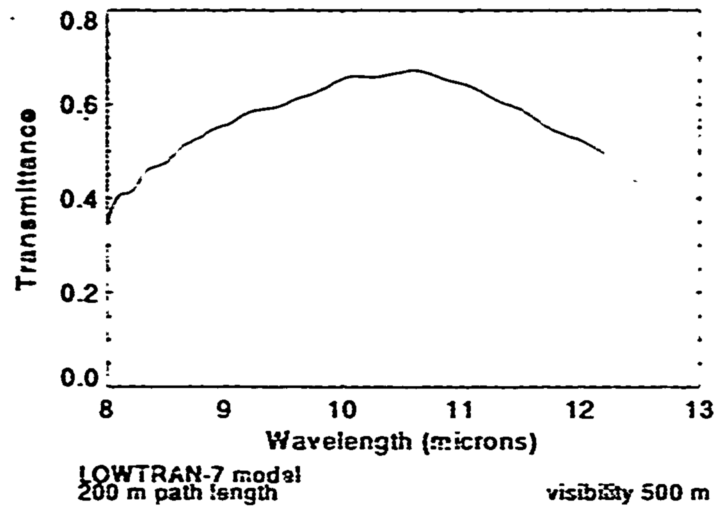

Figure 14: Moderate fog transmittance (LOWTRAN 7, far IR)

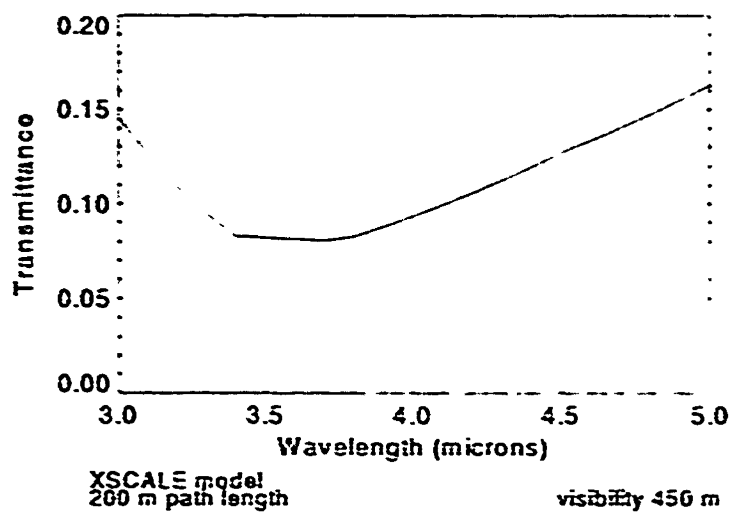

Figure 15: Moderate fog transmittance (XSCALE, mid IR)

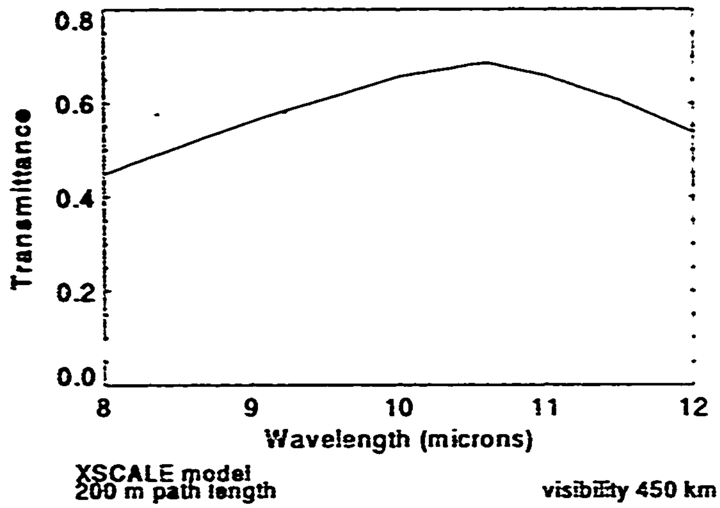

Figure 16: Moderate fog transmittance (XSCALE, far IR)

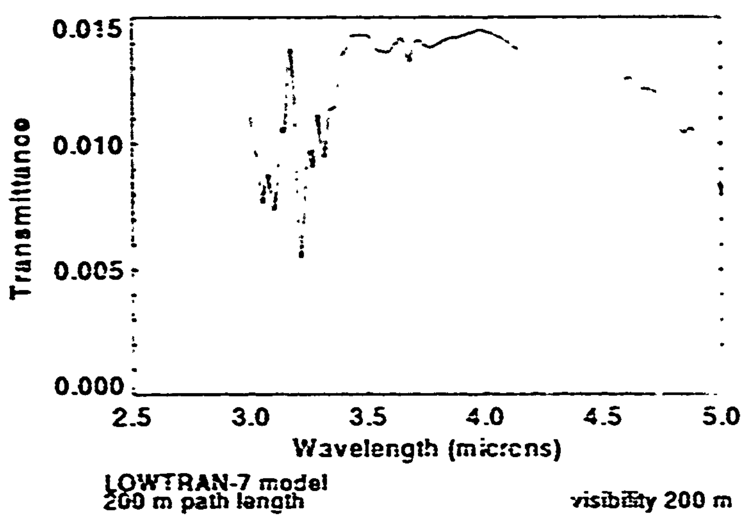

Figure 17: Heavy fog transmittance (LOWTRAN 7, mid IR)

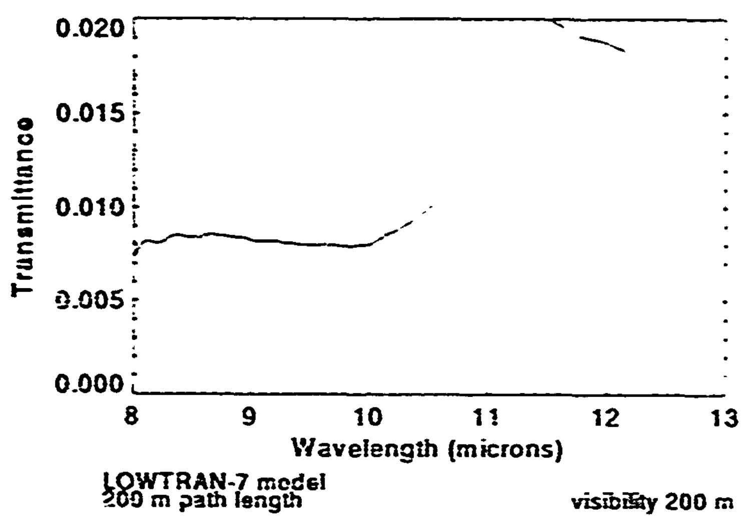

Figure 18: Heavy fog transmittance (LOWTRAN 7, far IR)

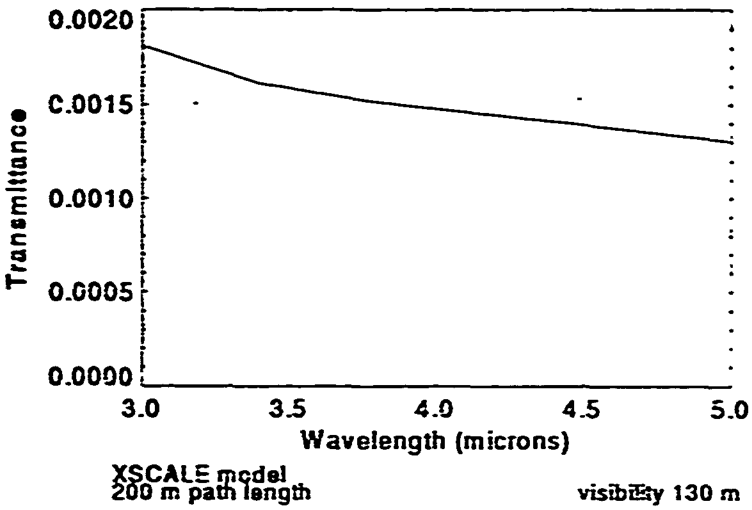

Figure 19: Heavy fog transmittance (XSCALE, mid IR)

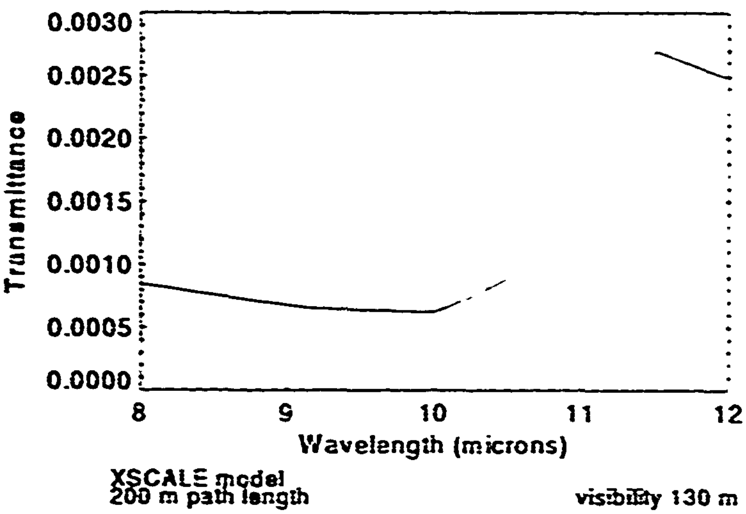

Figure 20: Heavy fog transmittance (XSCALE, far IR)

3.3 Heavy Dust Clouds

Some additional FCLOUD computer runs were made to calculate path radiance through a heavier dust cloud by using constant IR extinctions of 3.0 and 4.0 km^{-1}. This constant transmission is achieved by varying the mass-density of the dust at each wavelength. Figures 25 and 26 show the path radiance for an extinction of 3.0 km^{-1} and figures 27 and 28 show path radiance results for an extinction of 4.0 km^{-1}. These results are consistent with previous FCLOUD runs.

3.4 Multiple Scattering

The final FCLOUD runs involved the following changes in the computer input.

- Multiple scattering.
- Solar zenith angle of 15 degrees.
- 800-m path length.

Figures 29 and 30 show path radiance in which extinctions have been calculated by using PFNDAT. Figures 31 and 32 show path radiance results for an extinction of 3.0 km^{-1}. and figures 33 and 34 show path radiance for an extinction of 4.0 km^{-1}.

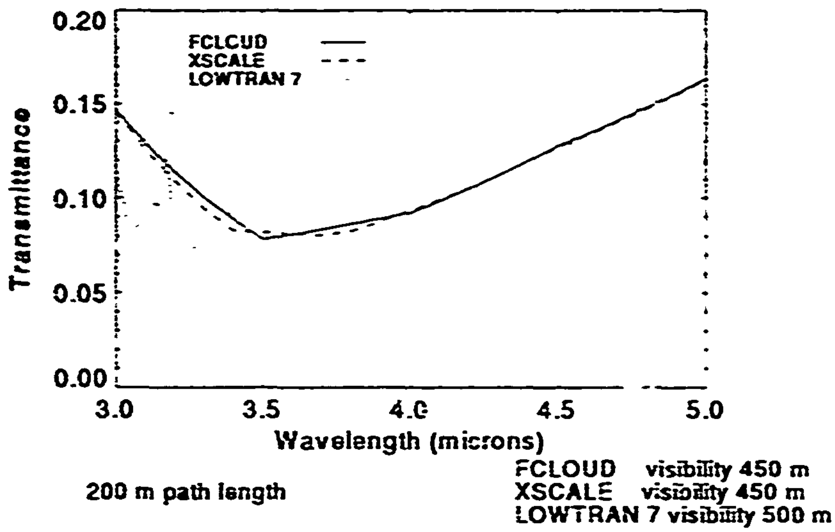

Figure 21: Comparison of moderate fog transmittances (mid IR)

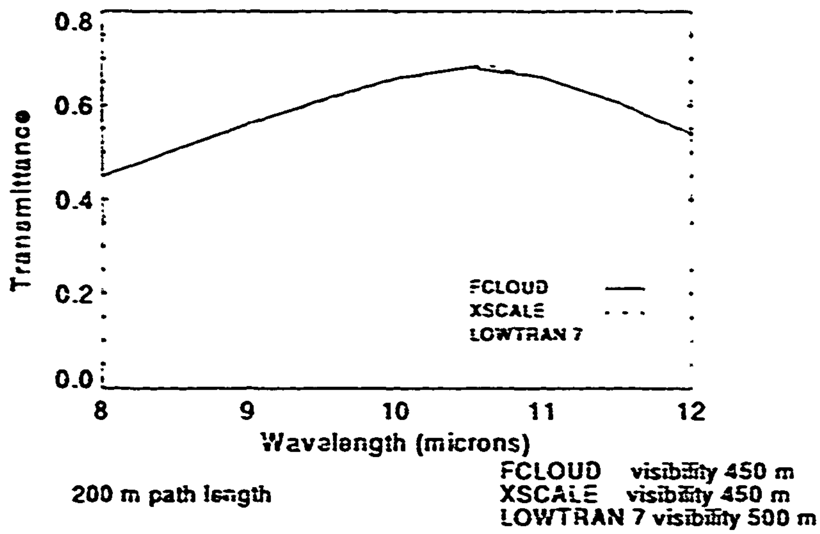

Figure 22: Comparison of moderate fog transmittances (far IR)

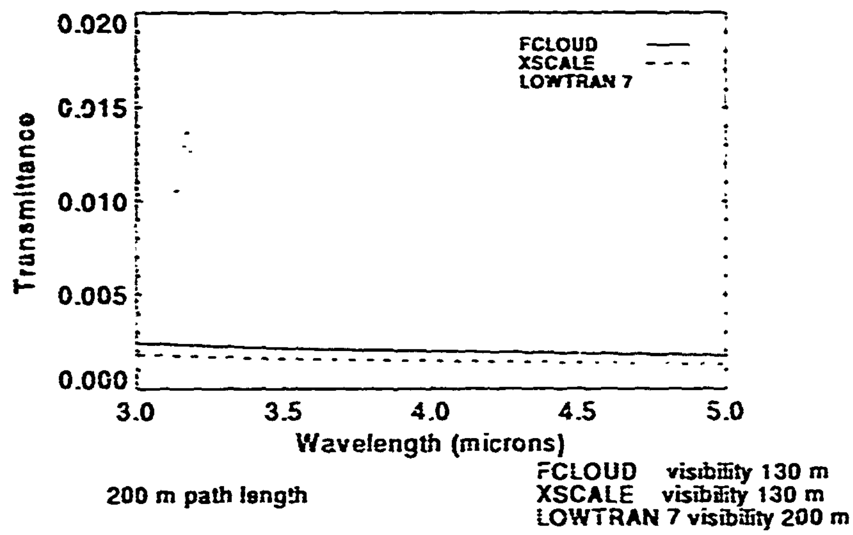

Figure 23: Comparison of heavy fog transmittances (mid IR)

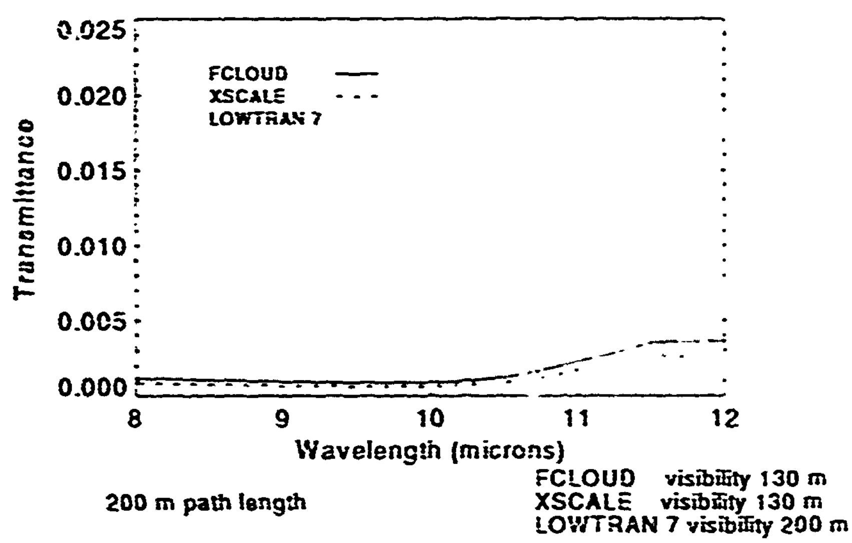

Figure 24: Comparison of heavy fog transmittances (far IR)

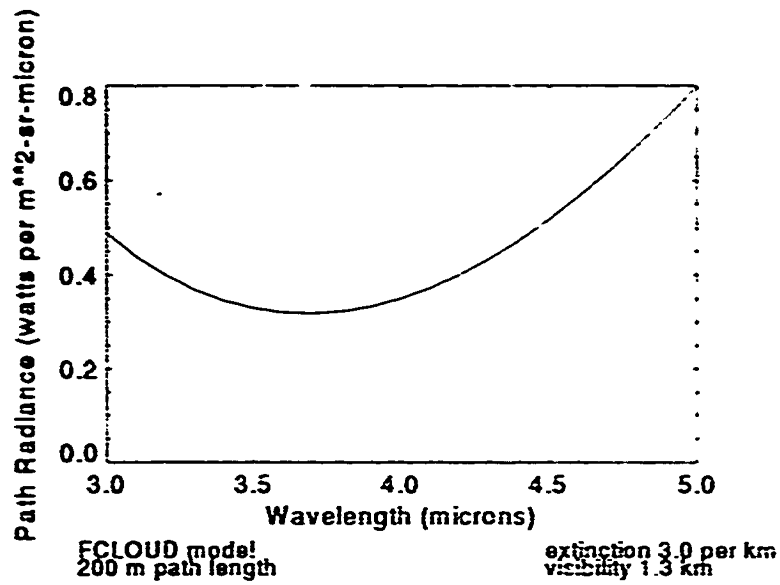

Figure 25: Dust path radiance (mid IR, $\sigma = 3.0\ \mathrm{km}^{-1}$)

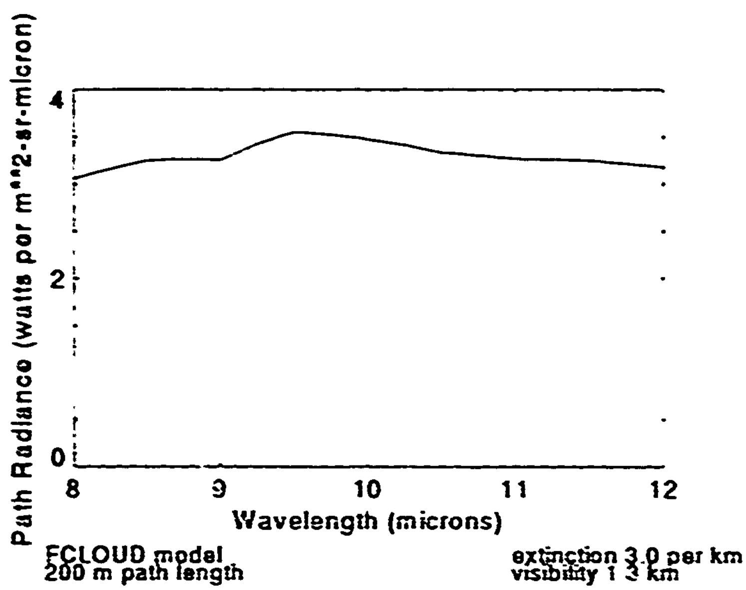

Figure 26: Dust path radiance (far IR, $\sigma = 3.0\ \mathrm{km}^{-1}$)

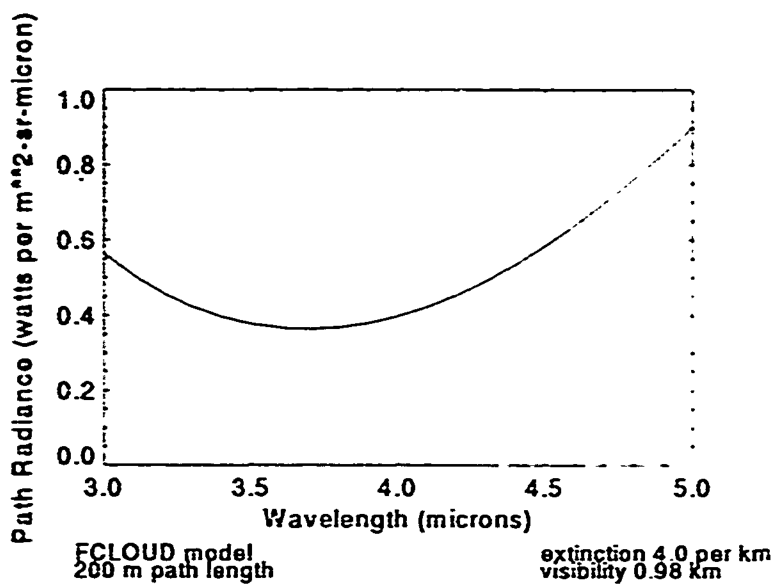

Figure 27: Dust path radiance (mid IR. $\sigma = 4.0\ km^{-1}$)

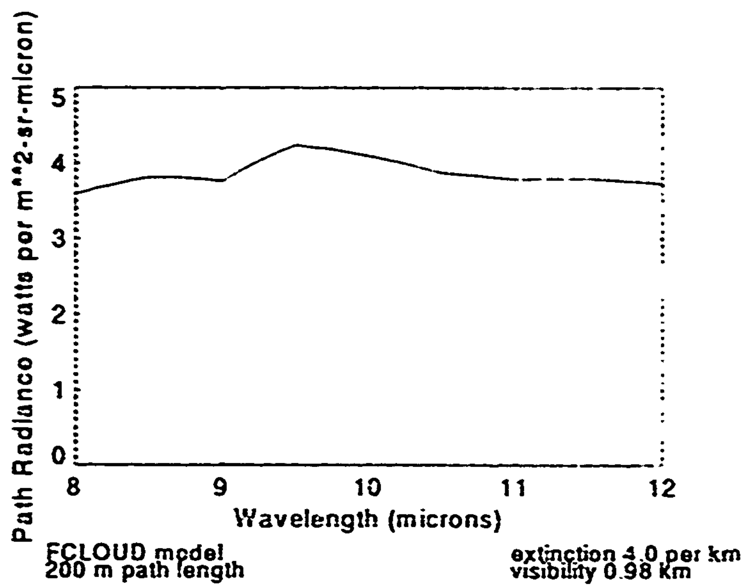

Figure 28: Dust path radiance (far IR. $\sigma = 4.0\ km^{-1}$)

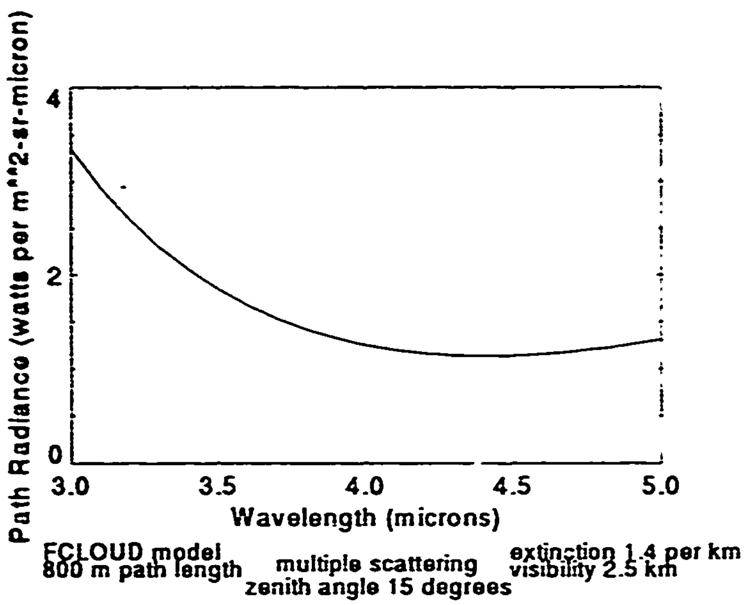

Figure 29: Dust path radiance (mid IR, $\sigma = 1.4$ km^{-1})

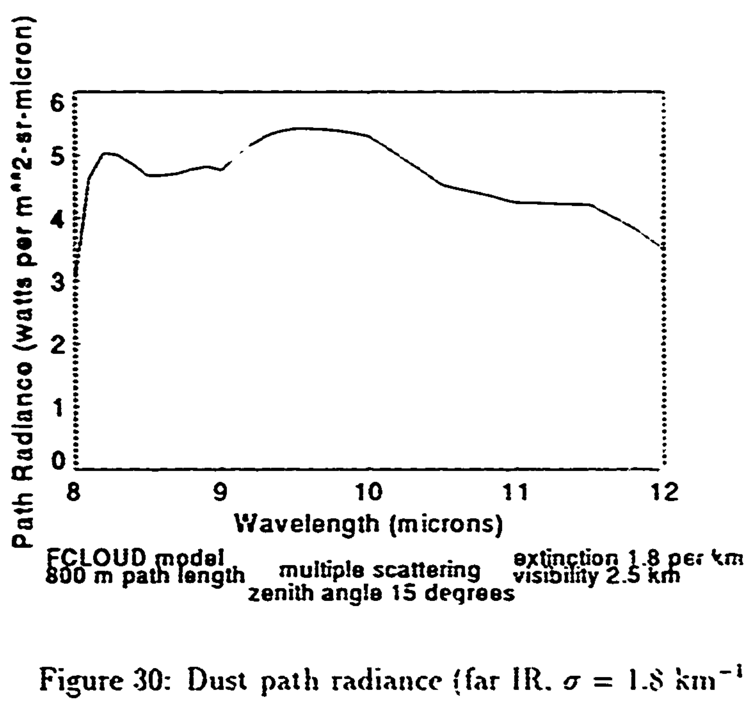

Figure 30: Dust path radiance (far IR, $\sigma = 1.8$ km^{-1})

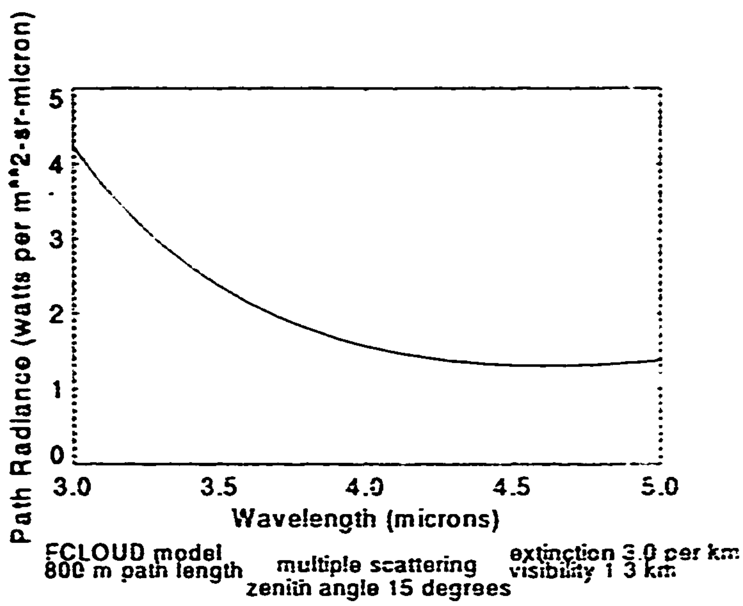

Figure 31: Dust path radiance (mid IR, $\sigma = 3.0\ km^{-1}$, 800 m path)

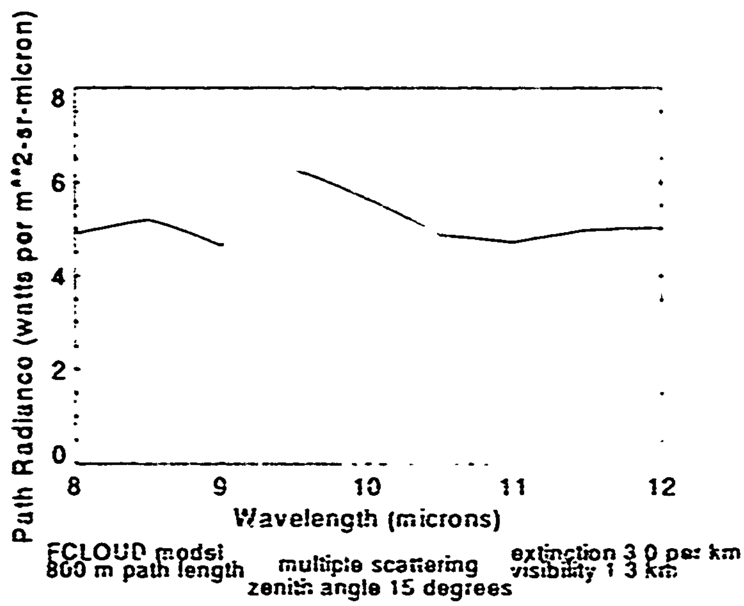

Figure 32: Dust path radiance (far IR, $\sigma = 3.0\ km^{-1}$, 800 m path)

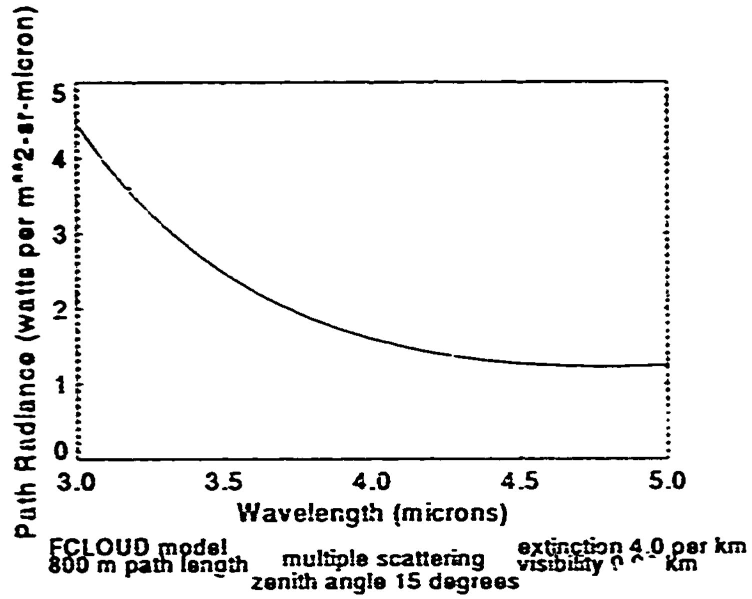

Figure 33: Dust path radiance (mid IR, $\sigma = 4.0\ km^{-1}$, 800 m path)

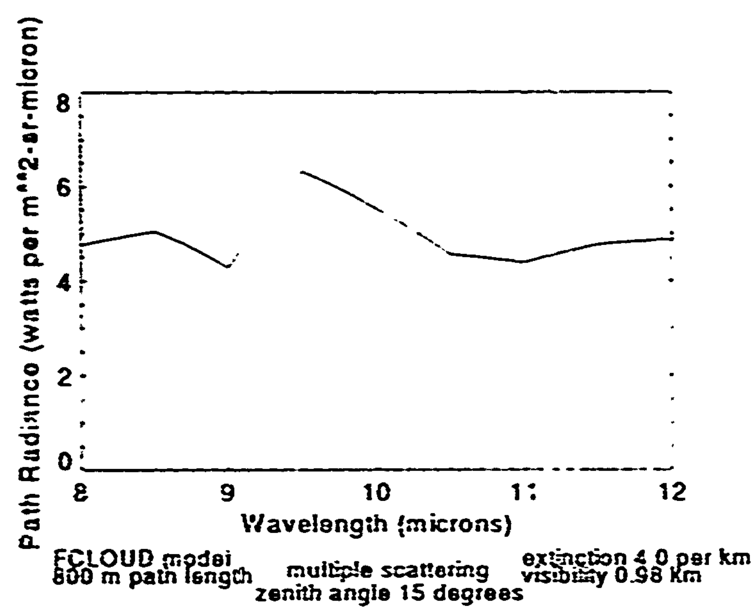

Figure 34: Dust path radiance (far IR, $\sigma = 4.0\ km^{-1}$, 800 m path)

4. Conclusions

This study investigated the effects of dust and fog in the 3- to 5-μm and 8- to 12-μm wavebands. The results show that IR transmission will be greatly attentuated in heavy fog and to a lesser extent in moderate fog. Output from the fog runs of the FCLOUD model is corroborated by both the LOWTRAN 7 and XSCALE models. A poor performance for an IR sensor under these conditions is anticipated.

The dust results were gathered from the FCLOUD model only. The highest IR transmission occurs when FCLOUD is run using extinctions as taken from PFNDAT (on average about 1.5 km^{-1}) for the single scattering case and a 200-m cloud. Attenuation is greatest for extinctions of 3.0 and 4.0 km^{-1} for the multiple scattering scenario with an 800-m cloud. As the dust loading becomes heavier (and extinction increases), the attenuation will become even more severe.

Literature Cited

Fiegel, R. P. 1992. *Natural Aerosol Extinction Module XSCALE92* (in preparation). U.S. Army Research Laboratory, White Sands Missile Range, NM.

Jennings, S. G., R. G. Pinnick, and H. J. Auvermann. 1978. Effects of Particulate Complex Refractive Index and Particle Size Distribution Variations on Atmospheric Extinction and Absorption for Visible through Middle IR Wavelengths, *Appl Opt* 17(24):3922-3929.

Kneizys, F. X., E. P. Shettle, L. W. Abreu, G. P. Anderson, J. H. Chetwynd, W. O. Gallery, J. E. A. Selby, and S. A. Clough. 1989. *Users Guide to LOWTRAN 7*, Air Force Geophysics Laboratory, Hanscom Air Force Base, MA.

Pinnick, R. G., G. Fernandez, and B. D. Hinds. 1983. Explosion Dust Particle Size Measurements. *Appl Opt* 22(1):95-102.

Shettle, E. P., and R. W. Fenn. 1979. *Models for the Aerosols of the Lower Atmosphere and the Effects of Humidity Variations on Their Optical Properties*. AFGL-TR-79-0214. Air Force Geophysics Laboratory, Hanscom Air Force Base, MA.

Shirkey, R. C., R. A. Sutherland, and M. A. Seagraves. 1987. *EOSAEL 87, Volume 26, Aerosol Phase Function Data Base PFNDAT*. ASL-TR-0221-26. U.S. Army Atmospheric Sciences Laboratory, White Sands Missile Range, NM.

Turner, R. E., 1987. *EOSAEL 87, Volume 18, Contrast Transmission Modules FCLOUD and OVRCST*. ASL-TR-0221-18. Science Applications Incorporated, Ann Arbor, MI. Prepared under contract for U.S. Army Atmospheric Sciences Laboratory, White Sands Missile Range, NM.

DISTRIBUTION LIST FOR PUBLIC RELEASE

Commandant
U.S. Army Chemical School
ATTN: ATZN-CM-CC (S. Barnes)
Fort McClellan, AL 36205-5020

Commander
U.S. Army Aviation Center
ATTN: ATZQ-D-MA
Mr. Oliver N. Heath
Fort Rucker, AL 36362

NASA/Marshall Space Flight Center
Deputy Director
Space Science Laboratory
Atmospheric Sciences Division
ATTN: E501 (Dr. George H. Fichtl)
Huntsville, AL 35802

NASA/Marshall Space Flight Center
Atmospheric Sciences Division
ATTN: Code ED-41
Huntsville, AL 35812

Deputy Commander
U.S. Army Strategic Defense Command
ATTN: CSSD-SL-L
Dr. Julius Q. Lilly
P.O. Box 1500
Huntsville, AL 35807-3801

Commander
U.S. Army Missile Command
ATTN: AMSMI-RD-AC-AD
Donald R. Peterson
Redstone Arsenal, AL 35898-5242

Commander
U.S. Army Missile Command
ATTN: AMSMI-RD-AS-SS
Huey F. Anderson
Redstone Arsenal, AL 35898-5253

Commander
U.S. Army Missile Command
ATTN: AMSMI-RD-AS-SS
B. Williams
Redstone Arsenal, AL 35898-5253

Commander
U.S. Army Missile Command
ATTN: AMSMI-RD-DE-SE
Gordon Lill, Jr.
Redstone Arsenal, AL 35898-5245

Commander
U.S. Army Missile Command
Redstone Scientific Information
Center
ATTN: AMSMI-RD-CS-R/Documents
Redstone, Arsenal, AL 35898-5241

Commander
U.S. Army Intelligence Center
and Fort Huachuca
ATTN: ATSI-CDC-C (Mr. Colanto)
Fort Huachuca, AZ 85613-7000

Northrup Corporation
Electronics Systems Division
ATTN: Dr. Richard D. Tooley
2301 West 120th Street, Box 5032
Hawthorne, CA 90251-5032

Commander - Code 3331
Naval Weapons Center
ATTN: Dr. Alexis Shlanta
China Lake, CA 93555

Commander
Pacific Missile Test Center
Geophysics Division
ATTN: Code 3250 (Terry E. Battalino)
Point Mugu, CA 93042-5000

Lockheed Missiles & Space Co., Inc.
Kenneth R. Hardy
Org/91-01 B/255
3251 Hanover Street
Palo Alto, CA 94304-1191

Commander
Naval Ocean Systems Center
ATTN: Code 54 (Dr. Juergen Richter)
San Diego, CA 92152-5000

Meteorologist in Charge
Kwajalein Missile Range
P.O. Box 67
APO San Francisco, CA 96555

U.S. Department of Commerce
Mountain Administration Support
Center
Library, R-51 Technical Reports
325 S. Broadway
Boulder, CO 80303

Dr. Hans J. Liebe
NTIA/ITS S 3
325 S. Broadway
Boulder, CO 80303

NCAR Library Serials
National Center for Atmos Rsch
P.O. Box 3000
Boulder, CO 80307-3000

HQDA
ATTN: DAMI-POI
Washington, DC 20310-1067

Mil Asst for Env Sci Ofc of
The Undersecretary of Defense
for Rsch & Engr/R&AT/E&LS
Pentagon - Room 3D129
Washington, DC 20301-3080

HQDA
DEAN-RMD/Dr. Gomez
Washington, DC 20314

Director
Division of Atmospheric Science
National Science Foundation
ATTN: Dr. Eugene W. Bierly
1800 G. Street, N.W.
Washington, DC 20550

Commander
Space & Naval Warfare System Command
ATTN: PMW-145-1G (LT Painter)
Washington, DC 20362-5100

Commandant
U.S. Army Infantry
ATTN: ATSH-CD-CS-OR
Dr. E. Dutoit
Fort Benning, GA 30905-5090

USAFETAC/DNE
Scott AFB, IL 62225

Air Weather Service
Technical Library - FL4414
Scott AFB, IL 62225-5458

USAFETAC/DNE
ATTN: Mr. Charles Glauber
Scott AFB, IL 62225-5008

Commander
U.S. Army Combined Arms Combat
ATTN: ATZL-CAW (LTC A. Kyle)
Fort Leavenworth, KS 66027-5300

Commander
U.S. Army Space Institute
ATTN: ATZI-SI (Maj Koepsell)
Fort Leavenworth, KS 66027-5300

Commander
U.S. Army Space Institute
ATTN: ATZL-SI-D
Fort Leavenworth, KS 66027-7300

Commander
Phillips Lab
ATTN: PL/LYP (Mr. Chisholm)
Hanscom AFB, MA 01731-5000

Director
Atmospheric Sciences Division
Geophysics Directorate
Phillips Lab
ATTN: Dr. Robert A. McClatchey
Hanscom AFB, MA 01731-5000

Raytheon Company
Dr. Charles M. Sonnenschein
Equipment Division
528 Boston Post Road
Sudbury, MA 01776
Mail Stop 1K9

Director
U.S. Army Materiel Systems
Analysis Activity
ATTN: AMXSY-MP (H. Cohen)
APG, MD 21005-5071

Commander
U.S. Army Chemical Rsch,
Dev & Engr Center
ATTN: SMCCR-OPA (Ronald Pennsyle)
APG, MD 21010-5423

Commander
U.S. Army Chemical Rsch,
Dev & Engr Center
ATTN: SMCCR-RS (Mr. Joseph Vervier)
APG, MD 21010-5423

Commander
U.S. Army Chemical Rsch,
Dev & Engr Center
ATTN: SMCCR-MUC (Mr. A. Van De Wal)
APG, MD 21010-5423

Director
U.S. Army Materiel Systems
Analysis Activity
ATTN: AMXSY-AT (Mr. Fred Campbell)
APG, MD 21005-5071

Director
U.S. Army Materiel Systems
Analysis Activity
ATTN: AMXSY-CR (Robert N. Marchetti)
APG, MD 21005-5071

Director
U.S. Army Materiel Systems
Analysis Activity
ATTN: AMXSY-CS (Mr. Brad W. Bradley)
APG, MD 21005-5071

Director
U.S. Army Research Laboratory
ATTN: AMSRL-D
2800 Powder Mill Road
Adelphi, MD 20783

Director
U.S. Army Research Laboratory
ATTN: AMSRL-OP-CI-A
(Technical Publishing)
2800 Powder Mill Road
Adelphi, MD 20783

Director
U.S. Army Research Laboratory
ATTN: AMSRL-OP-CI-AD, Record Copy
2800 Powder Mill Road
Adelphi, MD 20783

Director
U.S. Army Research Laboratory
ATTN: AMSRL-SS-SH
Dr. Z.G. Sztankay
2800 Powder Mill Road
Adelphi, MD 20783

National Security Agency
ATTN: W21 (Dr. Longbothum)
9800 Savage Road
Ft George G. Meade, MD 20755-6000

U. S. Army Space Technology
and Research Office
ATTN: Brenda Brathwaite
5321 Riggs Road
Gaithersburg, MD 20882

OIC-NAVSWC
Technical Library (Code E-232)
Silver Springs, MD 20903-5000

The Environmental Research
Institute of Michigan
ATTN: IRIA Library
P.O. Box 134001
Ann Arbor, MI 48113-4001

Commander
U.S. Army Research Office
ATTN: DRXRO-GS (Dr. W.A. Flood)
P.O. Box 12211
Research Triangle Park, NC 27709

Dr. Jerry Davis
North Carolina State University
Department of Marine, Earth, &
Atmospheric Sciences
P.O. Box 8208
Raleigh, NC 27650-8208

Commander
U. S. Army CECRL
ATTN: CECRL-RG (Dr. H. S. Boyne)
Hanover. NH 03755-1290

Commanding Officer
U.S. Army ARDEC
ATTN: SMCAR-IMI-I, Bldg 59
Dover, NJ 07806-5000

U.S. Army Communications-Electronics
Command EW/RSTA Directorate
ATTN: AMSEL-RD-EW-OP
Fort Monmouth, NJ 07703-5206

Commander
U.S. Army Satellite Comm Agency
ATTN: DRCPM-SC-3
Fort Monmouth, NJ 07703-5303

6585th TG (AFSC)
ATTN: RX (CPT Stein)
Holloman AFB, NM 88330

Department of the Air Force
OL/A 2nd Weather Squadron (MAC)
Holloman AFB, NM 88330-5000

PL/WE
Kirtland AFB, NM 87118-6008

Director
U.S. Army TRADOC Analysis Command
ATTN: ATRC-WSS-R
White Sands Missile Range, NM 88002

USAF Rome Laboratory Technical
Library, FL2810 Corridor W, Site 262,
RL//SUL (DOCUMENTS LIBRARY)
26 Electronics Parkway, Bldg 106
Griffiss AFB, NY 13441-4514

Department of the Air Force
7th Squadron
APO, NY 09403

AWS
USAREUR/AEAWX
APO, NY 09403-5000

AFMC/DOW
Wright-Patterson AFB, OH 0334-5000

Commandant
U.S. Army Field Artillery School
ATTN: ATSF-TSM-TA
Mr. Charles Taylor
Fort Sill, OK 73503-5600

Commander
Naval Air Development Center
ATTN: Al Salik (Code 5012)
Warminister, PA 18974

Commander
U.S. Army Dugway Proving Ground
ATTN: STEDP-MT-DA-M
Mr. Paul Carlson
Dugway, UT 84022

Commander
U.S. Army Dugway Proving Ground
ATTN: STEDP-MT-DA-L
Dugway, UT 84022

Commander
U.S. Army Dugway Proving Ground
ATTN: STEDP-MT-M (Mr. Bowers)
Dugway, UT 84022-5000

Defense Technical Information Center
ATTN: DTIC-FDAC (2)
Cameron Station
Alexandria, VA 22314

Commanding Officer
U.S. Army Foreign Science &
Technology Center
ATTN: CM
220 7th Street, NE
Charlottesville, VA 22901-5396

Naval Surface Weapons Center
Code G63
Dahlgren, VA 22448-5000

Commander
U.S. Army OEC
ATTN: CSTE-EFS
Park Center IV
4501 Ford Ave
Alexandria, VA 22302-1458

Commander and Director
U.S. Army Corps of Engineers
Engineer Topographics Laboratory
ATTN: ETL-GS-LB
Fort Belvoir, VA 22060

TAC/DOWP
Langley AFB, VA 23665-5524

U.S. Army Topo Engineering Center
ATTN: CETEC-ZC
Fort Belvoir, VA 22060-5546

Commander
Logistics Center
ATTN: ATCL-CE
Fort Lee, VA 23801-6000

Commander
USATRADOC
ATTN: ATCD-FA
Fort Monroe, VA 23651-5170

Science and Technology
101 Research Drive
Hampton, VA 23666-1340

Commander
U.S. Army Nuclear & Cml Agency
ATTN: MONA-ZB Bldg 2073
Springfield, VA 22150-3198

ERRATA FOR ARL-MR-35

INFRARED TRANSMISSION AND PATH RADIANCE THROUGH DUST AND FOG

Please change ARL report number of Infrared Transmission and Path Radiance Through Dust and Fog, April 1993, from ARL-MR-35 to ARL-MR-6. Please make this change on the front cover and also in box 8 on the SF 298, page 1 of the document.